

Three-dimensional analysis of eutectic grains in hypoeutectic Al–Si alloys

Cameron M. Dinnis, Arne K. Dahle*, John A. Taylor

*CRC for Cast Metals Manufacturing (CAST), Division of Materials Engineering, School of Engineering,
The University of Queensland, UDP Number 055, St. Lucia, Qld 4072, Australia*

Abstract

An approach to the qualitative analysis of quenched microstructures in three dimensions is presented and demonstrated on unmodified and Sr-modified Al–10% Si samples. The samples were repeatedly polished to obtain a series of digital images through the depth of the microstructure. A three-dimensional reconstruction of the microstructure was obtained by assembling the images of the serial sections. Reconstructions were made of unmodified and Sr-modified Al–Si eutectic grains that were quenched during eutectic solidification. The three-dimensional reconstructions show that strontium modification changes the size and morphology of the Al–Si eutectic grains. Sr-modified eutectic grains are large approximately spherical grains and grow with a high interface velocity. In the unmodified alloy, many small eutectic grains grow from the dendrite arm tips. The unmodified eutectic grains appear to grow from the dendrite tips into the undercooled liquid, rather than back-filling the dendrite envelope, possibly continuing to grow in the same manner as the equiaxed dendrites.

© 2004 Elsevier B.V. All rights reserved.

Keywords: Aluminium alloy; Serial sectioning; Al–Si eutectic

1. Introduction

1.1. The Al–Si eutectic

The Al–Si eutectic reaction is very important in the microstructural development of hypoeutectic Al–Si foundry alloys. Typically, the Al–Si eutectic accounts for a volume fraction of 50–90% of these alloys. Therefore, the solidification of the eutectic is most probably the major factor in determining the “as-cast” structure and properties of a component. This three-dimensional study of the Al–Si eutectic has been undertaken on unmodified and Sr-modified Al–10% Si alloys, in which the eutectic accounts for approximately three-quarters of the volume fraction.

Understanding the three-dimensional structure of eutectic grains may provide an insight into the processes occurring during eutectic nucleation and growth and ultimately lead to a better understanding of the properties of cast components. The three-dimensional structure of the eutectic silicon has

generally been observed with the aid of deep etching and electron microscopy; the work of Lu and Hellawell [1] is cited as an example. These methods are useful for fine-scale detail, such as determining the structure of the eutectic silicon, but not for examining the structure and morphology of the eutectic on the scale of eutectic grains.

Recent work, using electron backscatter diffraction (EBSD), has shown that the evolution of the Al–Si eutectic is dramatically altered by the addition of certain elements [2–10]. EBSD has allowed researchers to study crystallographic relationships between primary and eutectic aluminium and hence infer nucleation behaviour.

In unmodified alloys, the eutectic aluminium and the primary aluminium dendrites share crystallographic orientations [2–10]. This suggests that the eutectic grains nucleate adjacent to the primary dendrites. The orientation relationship is also present in ultra-high purity alloys modified by 150 ppm strontium [10] and in alloys with very high strontium levels (500 ppm) [3], but not in alloys of commercial purity modified with strontium levels typical of foundry practice [2,3,5–7]. The lack of a crystallographic relationship between primary and eutectic aluminium in typical Sr-modified

* Corresponding author. Tel.: +61 7 3365 4350; fax: +61 7 3365 3888.
E-mail address: a.dahle@minmet.uq.edu.au (A.K. Dahle).

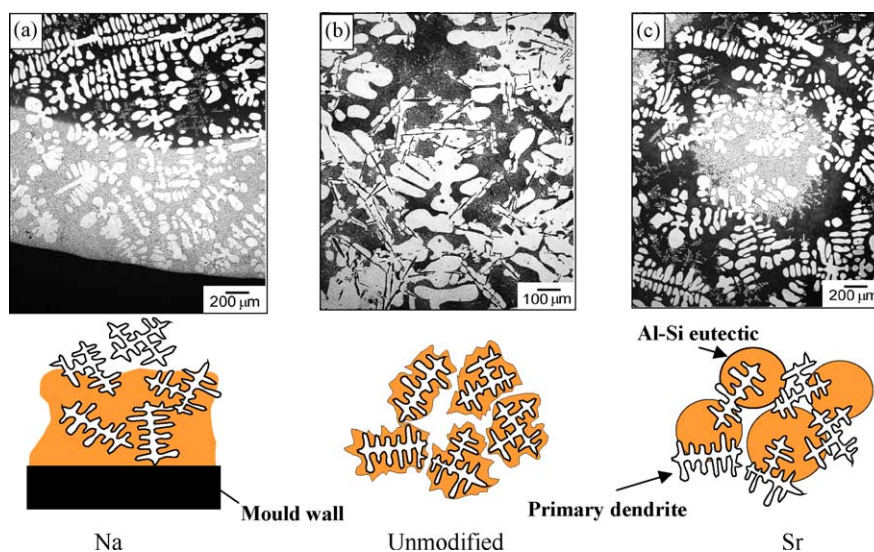


Fig. 1. Three possible eutectic growth morphologies: (a) planar-front growth opposite to the thermal gradient; (b) nucleation and growth on the primary Al dendrites; (c) independent heterogeneous nucleation and growth of eutectic grains in interdendritic spaces [3].

foundry alloys suggests that Sr-modified eutectic grains nucleate independently of the dendrites in the interdendritic liquid. In sodium-modified alloys, the eutectic nucleates at or near the mould wall and grows opposite to the direction of heat flow [8]. These growth modes are illustrated in Fig. 1.

1.2. Serial sectioning

In aluminium–silicon alloys, serial sectioning has been used to prove that the eutectic silicon crystals are connected plates or flakes [11] and to show the three-dimensional nature of the microstructure [12] and microporosity [13]. Until now, no work has been performed to investigate the three-dimensional form of the microstructure of Al–Si alloys during solidification, although the mushy zone of directionally solidified Pb–Sb alloys has been studied [14,15]. Serial sectioning has been coupled with three-dimensional visualisation software and used to study other alloy systems by developing three-dimensional views of the microstructure [16–21].

Some of these works [17–19] have shown that complete geometric and morphological information regarding a microstructure cannot be provided by two-dimensional metallographic analysis. In particular, information concerning connectivity cannot be obtained when observations are limited to two-dimensional metallographic sections. Serial sectioning is a useful method because it overcomes the problems associated with traditional two-dimensional metallographic techniques by providing information about microstructures in three-dimensions. However, as a metallographic tool, serial sectioning is not without problems. It is a time consuming and somewhat tedious procedure because it requires the repeated removal of layers of material, generally through grinding and polishing.

This work represents an interesting development in the analysis of the evolution of microstructural features during solidification, particularly Al–Si eutectic grains. It provides a method for determining and visualising three-dimensional shapes and structures and observing the relationship between microstructural features.

2. Experimental procedure

2.1. Preparation of the alloys

The evolution of the Al–Si eutectic was studied by partially solidifying samples before interrupting solidification by quenching. The quenched liquid solidifies with a very fine microstructure, allowing the portion of the sample that was liquid just prior to the quench to be distinguished from the portion that had already solidified.

The base metal used for the quenching procedure was a commercially pure (99.7%), non-grain-refined and unmodified aluminium ingot. Approximately 3 kg was placed in an electrical resistance furnace and brought to the molten state. The base metal was alloyed to 10% Si using foundry grade silicon. Where required, strontium was added to the melt, in the form of Al–10% Sr master alloy rod, to give a strontium concentration of approximately 200 ppm. The melt was allowed 1 h to equilibrate after reaching 750 °C, before the sampling procedure was begun.

Quench samples were made in small stainless-steel cups. The quench cups had dimensions of 22 mm external diameter, with a height of 57 mm, and a wall thickness of approximately 1.2 mm. Each cup was coated with a thin layer of boron nitride. The cups were immersed in the melt to a level just below the brim and allowed to equilibrate with the melt temperature before submerging. The cup was then removed from the melt

and a single, centrally located N-type thermocouple, with a stainless-steel sheath, was inserted to record the temperature of the solidifying sample. The cooling curves were displayed on the monitor of a personal computer. The unmodified sample was plunged into the quench bath approximately 45 s after eutectic nucleation was observed on the cooling curves. The strontium modified sample was plunged into the quench bath approximately 12 s after eutectic nucleation was observed on the cooling curves.

2.2. Serial sectioning

To obtain three-dimensional images of the microstructures the samples were subjected to serial sectioning. Serial sectioning involves the gradual removal of parallel layers of material and the imaging of each layer. Once the experimenter has become proficient at the procedure for sectioning and capturing the images, progress through the depth of the microstructure is relatively quick; approximately 12–15 min were required to complete each section. Nevertheless, a large amount of labour is required to produce a three-dimensional view of part of the microstructure (45 sections gave a depth of approximately 85 μm in the unmodified Al–10% Si alloy).

At present, three-dimensional images of microstructures are still novel, although the number of published examples cited in the introduction suggests their production and use is increasing.

The serial sectioning procedure for the quenched samples was executed through the following sequential steps:

1. The sample was mounted, ground and polished using standard metallographic techniques. An automatic polisher was used to polish the samples to a final polish with a 1 μm diamond suspension.
2. Two hardness indents were made on the surface of the specimen using a micro-hardness tester, spaced in such a way that they could be captured by the digital camera attached to the microscope. The indents were used to correctly align the images and also to measure the amount of material removed during each stage of the procedure. The geometry of the hardness indenter allows the depth of material removed in each sectioning operation to be calculated by comparing the length of the indent diagonals in successive sections.
3. The specimen was lightly polished again to remove the plastic deformation from the surface after the hardness indentations were made.
4. The diagonal lengths of the indents were measured to provide reference data for subsequent measurements.
5. Digital images of the two-dimensional microstructure were captured and stored for use in the three-dimensional reconstruction of the microstructure.
6. Material was removed from the surface of the specimen by re-polishing with a force of 35 N for a period of 3 min. The average depth of material removed by this step was 1.9 and 1.8 μm for the unmodified Al–10% Si and Sr-modified Al–10% Si alloy samples, respectively.
7. Steps 4–6 were repeated until the required depth of material had been removed, ensuring the same microstructural features were observed at each pass. The total depth of material removed was 85 and 117 μm for the unmodified Al–10% Si and Sr-modified Al–10% Si alloy samples, respectively. New hardness indents were made and recalibrated if the existing indents became too small.
8. The digital micrographs were then analysed, edited and assembled to yield three-dimensional microstructures with the help of an imaging software package. The three-dimensional microstructures were analysed to determine the shape and structure of the eutectic grains and the primary aluminium dendrites. The reconstruction and imaging procedure is presented in detail in the following section.

2.3. 3D reconstruction and imaging

The 3D reconstruction and image editing was performed using software developed by the Department of Biology at Boston University [22–24]. At the time of writing, this software was freely available at <http://synapses.bu.edu/tools/>. The digital images of the serial sections were converted to the required 8-bit greyscale format [22] and then edited using the image alignment program [23], ensuring exact alignment and superposition of the sections. Images were aligned by rotational and translational movements to match up the hardness indents and microstructural features. The aligned images of the serial sections were then imported to the three-dimensional reconstruction software [24] to enable phase boundaries and the solid/liquid interface position to be traced and stacked to render a three-dimensional projection.

The output of the software package is in the virtual reality modelling language (VRML) 1.0 format. The software used to edit and render the final three-dimensional images [25] cannot accept this file format, so the output was converted to a compatible format using a freeware program [26]. The three-dimensional images can be edited to adjust the transparency and colour of the phases.

Three features were reconstructed from the unmodified sample: primary aluminium, eutectic aluminium, and eutectic silicon. An estimate of the likely position of the boundary between the primary and eutectic aluminium was made by attempting to conform to the shape of the dendrite. It is acknowledged that this boundary is artificial because in unmodified hypoeutectic Al–Si alloys the eutectic aluminium shares crystallography with the primary aluminium due to epitaxial growth [2].

The reconstruction procedure did not have sufficient resolution to accurately capture the fibrous structure of the modified silicon. Therefore, only the primary aluminium and the Al–Si eutectic/quenched liquid interface were reconstructed in the Sr-modified sample.

3. Results

Example micrographs from the serial sections are presented in Fig. 2. The white phase is the aluminium, the black flake-like phase is the eutectic silicon and the very fine structure is the quenched liquid. In each case, a small region, shown outlined, was used to construct the three-dimensional model of the microstructure. Larger regions have been reconstructed, however, a smaller region allows greater focus on the features of interest and prevents the size of the model overwhelming the detail.

3.1. Unmodified Al–10% Si

In two-dimensional micrographs, it can appear as though some eutectic grains are independent of the primary dendrites. However, in three dimensions these apparently isolated eutectic grains are most likely connected to dendrite arms. In the captured volume, several instances of isolated eutectic grains were observed. In approximately half of these cases, further sectioning revealed a connection to the primary phase. It is likely that the remainder were connected to a dendrite above the original plane of sectioning.

Fig. 3 shows two views of the three-dimensional reconstruction of the region outlined in Fig. 2a. To aid visualisation of the reconstructed microstructure, the eutectic aluminium has been artificially distinguished from the primary aluminium. Five separate eutectic grains are present. Two of these are of substantial size, one is completely traversed by the serial sections (therefore, approximately 85 μm in size), and the other extends further into the sample (therefore, greater than 85 μm in size). The other three eutectic grains are small, appear only at the beginning and end of the series and consist of a single silicon crystal surrounded by aluminium.

The eutectic grains appear to grow from the tips of the dendrite arms rather than the base of the arms or trunk of the dendrites. Fig. 3a shows a polygonal Si crystal in contact with the primary dendrite arm. Most of the eutectic grains in the

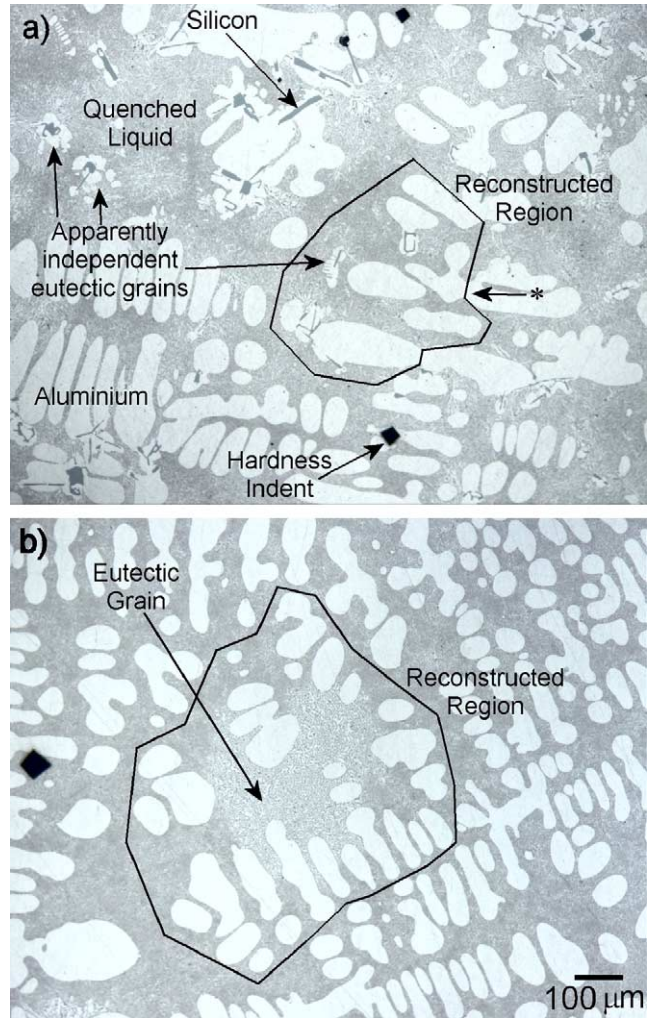


Fig. 2. Example micrographs from the serial sections. In each case, the outlined region is the region used to construct the three-dimensional model of the microstructure: (a) unmodified Al–10% Si alloy quenched approximately 45 s after the beginning of the eutectic solidification; (b) Sr-modified Al–10% Si alloy quenched approximately 12 s after the beginning of eutectic solidification. The white phase is aluminium. The dark grey flake-like phase in (a) is silicon. The fine grey structure is quenched liquid.

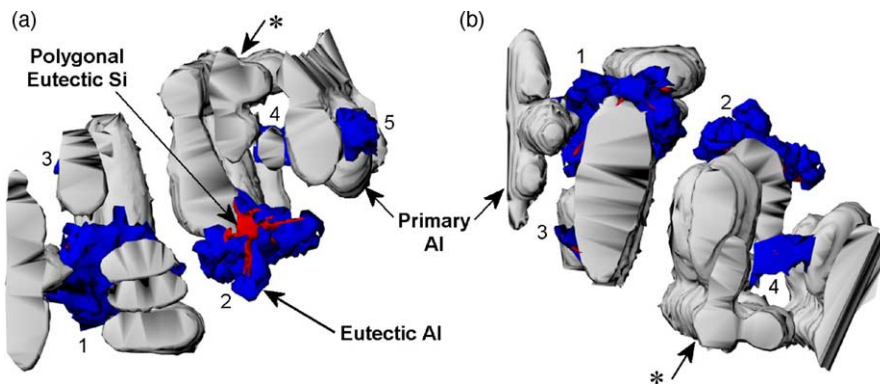


Fig. 3. Images of the three-dimensional reconstruction of the unmodified Al–10% Si samples quenched approximately 45 s after the beginning of the eutectic reaction: (a) shows the top, while (b) shows the underside of the three-dimensional reconstruction of the region shown in Fig. 2a.

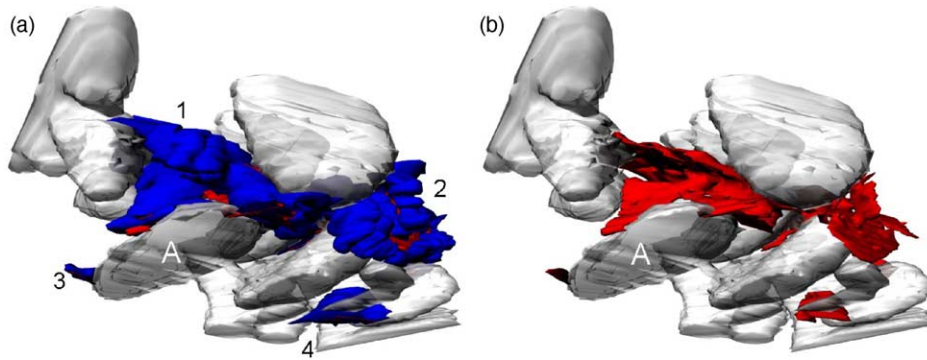


Fig. 4. (a) A eutectic grain (arrowed) growing from a dendrite tip into the intergranular liquid to span secondary dendrite arms. The eutectic grain has apparently grown from dendrite 1; (b) shows the same as (a) with the eutectic aluminium removed. The aluminium dendrites in the reconstructions have been rendered partially transparent to aid visualisation.

larger sectioned volume also form near the tips of dendrites. The eutectic grains seem to initially grow to span the tips of neighbouring dendrite arms, rather than “back-filling” the dendrite envelope by growing into the region deep between the arms.

Fig. 4 shows the reconstruction in a different orientation and reveals a eutectic grain (labelled 1) growing from the tip of a dendrite (labelled A) to span neighbouring dendrite tips. A second eutectic grain growing from a neighbouring dendrite tip (labelled 2) can also be seen in Fig. 4.

The eutectic silicon from the eutectic grain labelled 1 in Fig. 4 is presented in Fig. 5. A polygonal crystal can be seen at the centre of Fig. 5b. The eutectic silicon has most probably grown from this crystal. The silicon flakes form a continuous network, branching out from the polygonal crystal in three dimensions, apparently on well-defined planes. These planes most likely correspond to preferred growth directions for the silicon phase. Bridges between the silicon flakes are evident in Fig. 5c. These bridges may result from a branch of one flake having its growth arrested as it impinges upon a neighbouring flake.

3.2. Sr-modified Al–10% Si

A comparison of Figs. 4 and 6 reveals that the eutectic grain in the Sr-modified alloys bears no morphological resemblance to the unmodified eutectic grains. The Sr-modified sample was quenched much earlier (12 s) than the unmodified sample (45 s) because of amount of serial sectioning and reconstruction work posed by the large size of the eutectic grains in Sr-modified sample quenched 45 s after the beginning of eutectic solidification.

The fibrous eutectic silicon was too fine to reconstruct separately from the eutectic aluminium. The Sr-modified eutectic grain appears to grow around the dendrite arms, filling up the dendrite envelope, rather than growing from the dendrite tips. The reconstruction is approximately 117 μm deep and shows that the Sr-modified eutectic grain is roughly spherical.

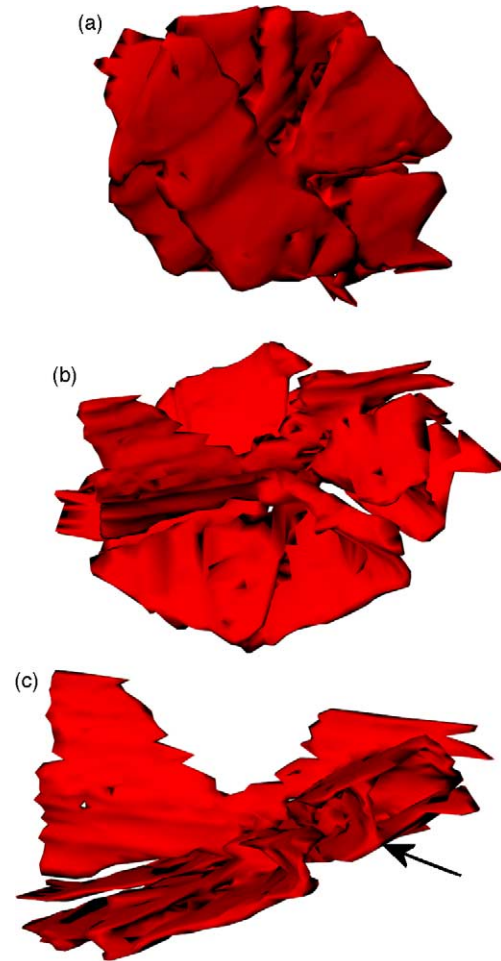


Fig. 5. (a)–(c) show reconstructed views of the silicon within the eutectic grain shown in Fig. 4. The silicon has apparently grown from a polygonal crystal that can be seen in the centre of (b), while bridges (arrowed) between flakes can be seen in (c). The ragged edges on some silicon flakes are a result of the difficulty in exactly matching phase boundaries in successive sections.

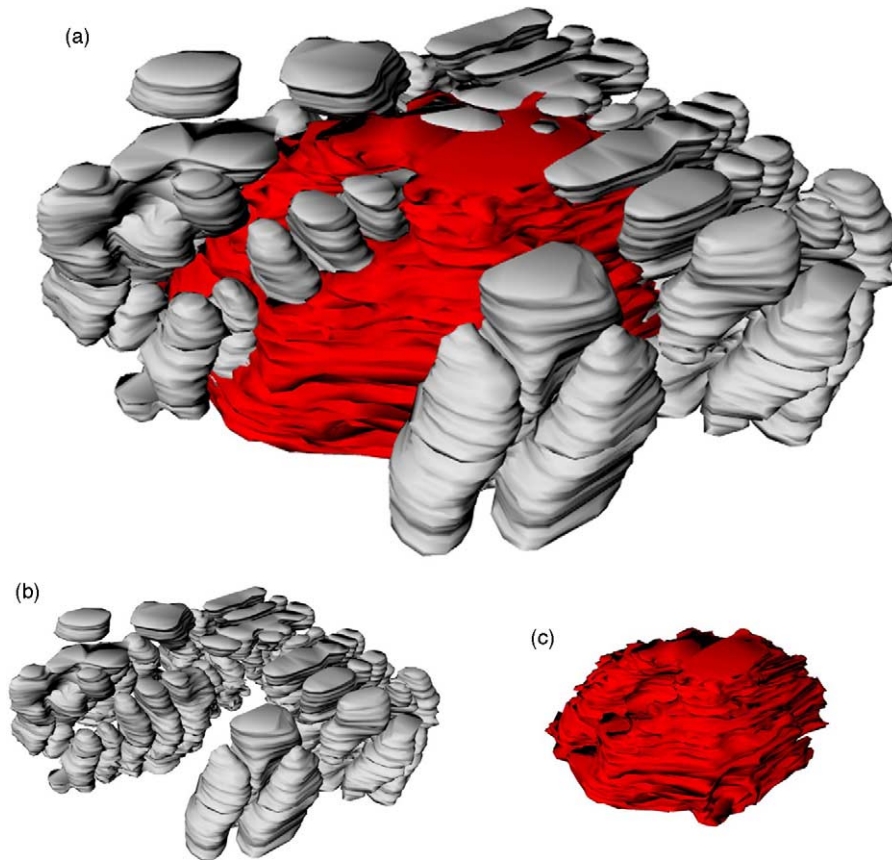


Fig. 6. (a) Three-dimensional reconstruction of an Al–10% Si alloy modified with 200 ppm Sr, quenched approximately 12 s after the beginning of the eutectic reaction. The eutectic grain is red and primary aluminium dendrites are grey; (b) and (c) show the same view with only the aluminium dendrites and the Sr-modified eutectic grain, respectively. Note (b) and (c) are shown at a smaller scale than (a).

4. Discussion

The reconstruction software is unable to exactly replicate the microstructure because it does not allow for different depths of material removal between sections. The reconstruction software applies an average distance between sections to determine the three-dimensional form of the object. This minor problem could be overcome with a commercial computer aided drafting (CAD) package with 3D capabilities or a more sophisticated image editing software package.

The continuous surface of the three-dimensional model is calculated from a series of discrete sections. In combination with slight errors in alignment between the sections and the difference between actual depth and calculated depth, this can lead to the appearance of steps in the reconstruction of curved surfaces. These steps are present in the reconstructions presented in this paper and are not considered a problem for qualitative analysis. Finer vertical resolution, i.e. smaller depth removed per section, would be one way to reduce the appearance of these steps, however, the extra work is believed to be unnecessary to produce three-dimensional microstructures for the purpose of qualitative analysis. The present combination of serial sectioning and software packages provides an accessible and low-cost means

to give indicative three-dimensional views of the microstructure.

4.1. Unmodified Al–10% Si

The depth of the reconstruction of the unmodified sample is approximately 85 μm . The sample was quenched approximately 45 s after eutectic nucleation. Therefore, assuming the eutectic grains nucleated when nucleation was detected on the cooling curves, the eutectic grain in Fig. 4 has grown with an average radial velocity of the order of 1 $\mu\text{m/s}$ to reach a diameter of approximately 80 μm .

Eutectic silicon nucleates on AIP particles [27]. These are readily available because the phosphorous level of most commercial alloys is in the range of 10–20 ppm. The particles are small and unwetted by aluminium and are most likely pushed ahead of the evolving solid/liquid interface. If it is assumed that AIP particles are randomly distributed throughout the melt, the most likely part of the dendrite to achieve favourable conditions for eutectic nucleation (i.e. an AIP particle adjacent to the interface, appropriate silicon concentration and sufficient undercooling) is the growing dendrite tip, since dendrites grow by the advance of the solid/liquid interface at the tips rather than the trunk.

For nucleation to occur adjacent to the dendrite trunk between two dendrite arms requires an AIP particle to be located adjacent to the relatively stationary solid/liquid interface. The base region between two dendrite arms forms a hyperbolic paraboloid (saddle) and would be, therefore, only marginally more thermodynamically favourable for nucleation than the tip. On the other hand, for nucleation to occur adjacent to the dendrite tip, an AIP particle needs to be located adjacent to the tip at the stage during solidification when eutectic nucleation is favourable.

The volume in which eutectic nucleation may occur is much larger for the tip than the base. For the dendrite trunk, the volume in which eutectic nucleation may occur forms the region immediately surrounding the trunk. On the other hand, the volume in which eutectic may nucleate on the dendrite tip includes the volume the tip will grow into. Therefore, when AIP particles are distributed randomly in the melt, the probability of eutectic nucleation is higher at the dendrite tip than the trunk.

In these samples, the aluminium dendrites solidify in an equiaxed manner and therefore, a local thermal gradient is expected in the liquid ahead of the interface. It is probable that a eutectic grain that nucleates adjacent to a dendrite tip growing into undercooled liquid will also grow into undercooled liquid. Alternatively, if the coherent network of aluminium dendrites is more thermally conductive than the residual liquid (and therefore, at a lower temperature), the eutectic grains will grow in a pseudo-columnar manner opposite the direction of heat flow. In the immediate vicinity of the dendrite, heat transfer occurs perpendicular to the surface of the dendrites (i.e. perpendicular to the curvature of the solid/liquid interface). Therefore, the eutectic grains will initially grow away from the dendrite arms.

Either way, after nucleating on an AIP particle, the silicon grows along the preferred crystallographic planes, par-

tituting aluminium and other elements into the liquid. The liquid surrounding the silicon particle is thereby enriched in aluminium. The eutectic aluminium grows epitaxially on the adjacent dendrite tip into the aluminium enriched liquid around the silicon flake. Thus, the silicon flakes control the shape of the eutectic/liquid interface.

4.2. Sr-modified Al–10% Si

The eutectic grains in Sr-modified alloys are roughly spherical before impingement with other eutectic grains (Fig. 6). The eutectic grain diameter can be estimated by using a simple geometrical construction. If the top and bottom surfaces of the reconstruction are assumed to be parallel sections through a sphere, a diameter can be determined as shown in Fig. 7a. The top surface of the sectioned eutectic grain has a diameter of approximately 192 μm and the bottom surface has a diameter of approximately 466 μm . These two surfaces are approximately 117 μm apart. Therefore, the eutectic grain has a diameter of approximately 538 μm . Fig. 7b shows a sphere of $\text{\O}538 \mu\text{m}$ superimposed over the reconstruction of the eutectic grain. The editing and rendering software [25] was used to position the sphere according to the geometry of Fig. 7a. The actual grain is slightly elongated in one direction (egg-shaped) and therefore, departs slightly from perfect spheroidicity. A localised temperature gradient within the liquid may be responsible for the departure from spheroidicity [28]. Alternatively, the grain may depart from spheroidicity after it impinges on aluminium dendrites. After impingement on the dendrites, the eutectic grain cannot grow freely in all directions. Therefore, to maintain a constant overall solid/liquid interface velocity, the eutectic grain is required to grow faster in some directions than others.

The Sr-modified sample was quenched approximately 12 s after eutectic nucleation. Therefore, assuming the eutectic

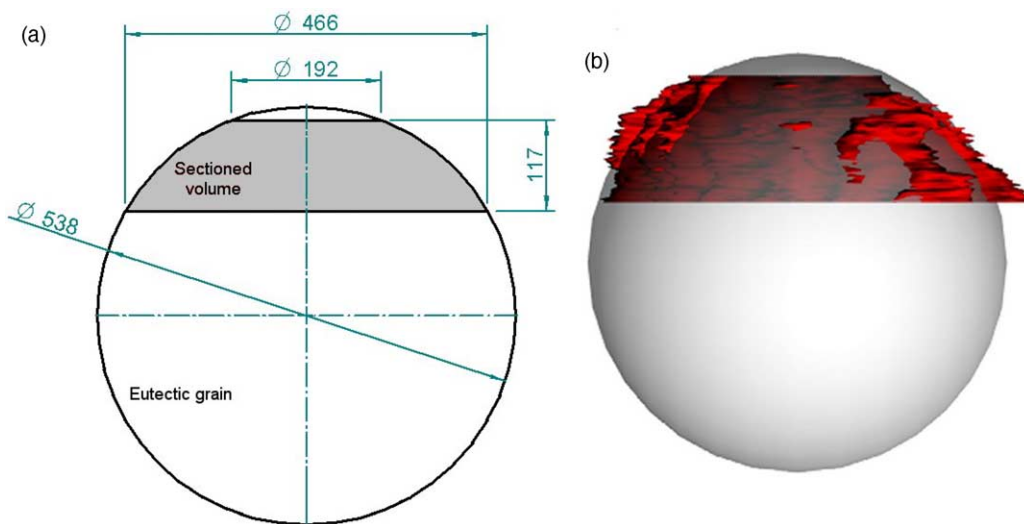


Fig. 7. (a) Geometrical construction to give an estimate of the diameter of the quenched Sr-modified eutectic grain. The top and bottom surfaces of the eutectic grain have been assumed circular and a sphere has been geometrically fitted to give an estimate of the eutectic grain diameter. (b) Sphere of $\text{\O}538 \mu\text{m}$ fitted to the reconstructed eutectic grain. The eutectic grain is not perfectly spherical.

grain nucleated at the time nucleation was detected on the cooling curves, the grain has grown with an average radial velocity of approximately 22 $\mu\text{m/s}$ to reach a diameter of 538 μm . McDonald et al. [29,30] have presented a model to describe the growth of Sr-modified eutectic grains. The grain radius, R , of a grain growing for a period of time, t , after nucleation at time t_n , can be calculated from the growth velocity, V , and the undercooling measured on the cooling curves, ΔT , via Eqs. (1) and (2) [29,30]:

$$V = 0.33 \Delta T^2 \quad (1)$$

$$R(t) = \int_{t_n}^t V dt = \int_{t_n}^t 0.33 \Delta T^2 dt \quad (2)$$

Applying these equations to the cooling curve data gives a eutectic grain diameter of approximately 160 μm at the time of quenching, with an average radial velocity of approximately 7 $\mu\text{m/s}$. The model and the measurements differ by a factor of 3, which is probably a reasonable fit given the assumptions of the model and the errors of the geometrical estimation.

The growth model of McDonald et al. [29,30] implicitly assumes steady-state solidification of a planar interface in a positive temperature gradient because the growth equations were derived from directional solidification experiments. During equiaxed solidification, these conditions are violated, allowing the model to be accurate only within an order of magnitude [30]. There are also difficulties with estimating the nucleation temperature and time of a single eutectic grain from the cooling curves measured for the bulk sample.

There are also inherent uncertainties involved with using the geometrical estimate of the eutectic grain size. The cross-sections of the eutectic grain on the micrographs are only approximately circular and therefore, the diameters used in the geometrical construction must be estimated from a circle that provides a reasonable fit to the cross-section of the eutectic grain. The sensitivity of the geometrically estimated grain size to the cross-section diameter is also dependent on the depth of material between the top and bottom sections. The larger the sectioned volume is in proportion to the volume of the estimated sphere, the more accurate the geometrical grain size estimate.

However, the results presented here do support the conclusions of McDonald et al. [29,30] that Sr-modified eutectic grains are approximately an order of magnitude larger than unmodified eutectic grains, grow with a much higher interface velocity and solidify with a different spatial distribution.

This serial sectioning method may be adapted to help identify possible nucleant particles for the Sr-modified eutectic grains. The geometrical construction of Fig. 7a would allow the equatorial regions of the eutectic grain to be located and examined. After an initial section has been examined, a large sectioning step (of the order of 50–100 μm , or more) would allow the depth within the eutectic grain to be determined in accordance with the geometry of (a). Once it had been established that the section was near an (Fig. 7) equatorial plane of

the grain, small sectioning steps could be performed to look for a possible nucleant particle.

5. Conclusions

An investigation of the three-dimensional nature of certain microstructural features of Al–Si alloys has been conducted. The reconstructed serial sections show that the eutectic grains in unmodified Al–10% Si alloys grow from the tips of the primary aluminium dendrites. In the early stages of eutectic solidification, the eutectic grains were observed to grow into the intergranular liquid and span secondary dendrite arm tips rather than back-filling the dendrite envelope by growing deep between secondary dendrite arms. The eutectic silicon was observed to form a continuous branched network of flakes, apparently growing on well-defined planes.

The Sr-modified eutectic grain was observed to be significantly larger than the unmodified eutectic grains, despite being quenched at a much earlier stage during the eutectic reaction. An estimate of the diameter of the approximately spherical Sr-modified eutectic grain was calculated, based on a simple geometrical construction, from the diameter of the top and bottom surfaces of the sectioned grain.

Serial sectioning was found to be a useful, although time and labour intensive, method to produce three-dimensional images of microstructures. The use of the serial sectioning technique on quenched samples has proved to be a constructive means to investigate the microstructure during solidification. The combination of software packages described provides an inexpensive means to produce indicative three-dimensional views of metallic microstructures.

Acknowledgements

The authors would like to acknowledge the financial support of the Cooperative Research Centre for Cast Metals Manufacturing (CAST). CAST was established and is funded in part by the Australian Government's Cooperative Research Centres Program.

References

- [1] S.-Z. Lu, A. Hellawell, *Metall. Trans. A* 18A (1987) 1721–1733.
- [2] A.K. Dahle, J. Hjelen, L. Arnberg, Proceedings of the 4th Decennial International Conference on Solidification Processing, 1997, pp. 527–530.
- [3] A.K. Dahle, K. Nogita, J.W. Zindel, S.D. McDonald, L.M. Hogan, *Metall. Mater. Trans. A* 32A (2001) 949–960.
- [4] A.K. Dahle, J.A. Taylor, D.A. Graham, *Aluminum Trans.* 3 (2000) 17–30.
- [5] K. Nogita, A.K. Dahle, *Mater. Trans. JIM* 42 (2001) 207–214.
- [6] K. Nogita, A.K. Dahle, *Mater. Trans. JIM* 42 (2001) 393–396.
- [7] K. Nogita, A.K. Dahle, *Mater. Charact.* 46 (2001) 305–310.
- [8] K. Nogita, S.D. McDonald, J.W. Zindel, A.K. Dahle, *Mater. Trans. JIM* 42 (2001) 1981–1986.

- [9] K. Nogita, A. Knuutinen, S.D. McDonald, A.K. Dahle, *J. Light Met.* 1 (2001) 219–228.
- [10] G. Heiberg, L. Arnberg, *J. Light Met.* 1 (2001) 43–49.
- [11] S. Ghosh, V. Kondic, *AFS Trans.* 71 (1963) 17–25.
- [12] J. Alkemper, P.W. Voorhees, *J. Microsc.* 201 (2001) 388–394.
- [13] M. Dighe, A. Tewari, G. Patel, T.G. Mirabelli, A.M. Gokhale, *AFS Trans.* 107 (1999) 353–356.
- [14] L. Yu, G.L. Ding, J. Reye, S.N. Ojha, S.N. Tewari, *Metall. Mater. Trans. A* 30 (1999) 2463–2472.
- [15] L. Yu, G.L. Ding, J. Reye, S.N. Tewari, S.N. Ojha, *Metall. Mater. Trans. A* 31 (2000) 2275A–2285A.
- [16] M. Li, et al., *Mater. Charact.* 41 (1998) 81–95.
- [17] M.V. Kral, G. Spanos, *Acta Mater.* 47 (1999) 711–724.
- [18] B. Niroumand, K. Xia, *Mater. Sci. Eng. A* 283 (2000) 70–75.
- [19] A. Tewari, A.M. Gokhale, *Mater. Charact.* 44 (2000) 259–269.
- [20] J. Alkemper, P.W. Voorhees, *Acta Mater.* 49 (2001) 897–902.
- [21] R. Mendoza, J. Alkemper, P.W. Voorhees, *Metall. Mater. Trans. A* 34 (2003) 481–489.
- [22] J.C. Fiala, *Convert*, 1.11b, Boston University, 2001.
- [23] J.C. Fiala, *Sem Align*, 1.26b, Boston University, 2001.
- [24] J.C. Fiala, *Igltrace*, 1.26b, Boston University, 2001.
- [25] R. McNeel, et al., *Rhinoceros*, 3.0 SR2, 2003.
- [26] K. Rule, *Crossroads*, 1.0, 1998.
- [27] K. Nogita, K. Tsujimoto, A.K. Dahle, J. Drennan, *Proceedings of the 18th Australian Conference on Electron Microscopy*, 2004, p. 52.
- [28] M. Rappaz, C. Charbon, R. Sasikumar, *Acta Metall. Mater.* 42 (1994) 2365–2374.
- [29] S.D. McDonald, A.K. Dahle, J.A. Taylor, D.H. St John, *Metall. Mater. Trans. A* 35A (2004) 1829–1837.
- [30] S.D. McDonald, *Eutectic solidification and porosity formation in unmodified and modified hypoeutectic aluminium–silicon alloys*, Ph.D. Thesis, Division of Materials Engineering, University of Queensland, 2003.